Signatures of multigap superconductivity in tunneling spectroscopy

Y. Noat, T. Cren, F. Debontridder, and D. Roditchev
Institut des Nanosciences de Paris, Université Pierre et Marie Curie—Paris 6, CNRS UMR 7588, Campus Boucicaut, 140 rue de Lourmel, F-75015 Paris, France

W. Sacks
Institut de Minéralogie et de Physique des Milieux Condensés, Université Pierre et Marie Curie—Paris 6, CNRS UMR 7590, Campus Boucicaut, 140 rue de Lourmel, F-75015 Paris, France

P. Toulemonde and A. San Miguel
Institut Néel, CNRS UPR 2940, Université Joseph Fourier, 25 Avenue des Martyrs, BP 166, F-38042 Grenoble Cedex 9, France and Université de Lyon, Laboratoire PMCN, CNRS, UMR 5586, Université Lyon 1, Villeurbanne 69622, France
(Received 16 December 2009; revised manuscript received 4 June 2010; published 26 July 2010; corrected 6 October 2010)

We considered a two-band superconductor with a nonzero interband quasiparticle coupling and numerically generated partial elementary excitation spectra for each band. These show deviations from the conventional Bardeen, Cooper, and Schrieffer form, resulting in characteristic signatures in the partial tunneling spectra. The total (measurable) tunneling spectra are calculated considering the **k** selection in the tunneling process. Due to the thermal smearing, the relevant spectral signatures may not be resolved in superconductor-insulator-normal-metal tunneling while they are clearly revealed in superconductor-insulator-superconductor (SIS) geometry. As an example, the excitation spectrum of 2H-$NbSe_2$ is considered in the framework of the developed tunneling model. A remarkable agreement obtained with the experimental SIS data suggests the material to be a two-band superconductor rather than an anisotropic one.

DOI: 10.1103/PhysRevB.82.014531 PACS number(s): 74.25.Gz

I. INTRODUCTION

In their original description of superconductivity, Bardeen, Cooper, and Schrieffer (BCS) introduced an isotropic and constant electron-electron attractive potential.[1] It is impressive how this simple approximation has been so successful to explain the basic properties of conventional superconductors (SCs) and specifically, their excitation spectrum (also often called "SC density of states," SC DOS). However, looking deeper into detail, some conventional SCs show deviations from the BCS model, a subject which has attracted considerable attention. The anisotropy of the pair potential[2] and strong-coupling effects, such as for Pb, result in sharp deviations of the SC DOS from the simple BCS model.[3,4] Still, among the departures from BCS, multigap SC has captured much interest, especially since the recent discovery of MgB_2 (Ref. 5) displaying a clear double gap in its spectrum.[6–8]

The two-band superconductivity was first theoretically studied by Suhl *et al.*[9] who proposed a simple extension of the one-band BCS model to the case of a material with two energy bands crossing the Fermi level. Already in the late 1960s the A15 family of SCs, such as V_3Si, revealed anomalies in the specific heat that could be attributed to the presence of several energy gaps.[10] The existence of two energy gaps had also been suggested for Nb, Ta, and V,[11] but the discovery of MgB_2 boosted the interest to multigap SC, not only due to the high T_c of MgB_2, but also because the two gaps in this material were clearly resolved with various techniques including specific-heat measurements[6] and tunneling spectroscopies,[7,8,12–14] those results being largely supported by theory (Refs. 15–17, and references therein).

Since MgB_2, other SCs are now supposed to be multigap or at least highly anisotropic. Even such a "standard" material as 2H-$NbSe_2$ considered over decades as a conventional anisotropic SC,[18,19] has been revisited. Many groups followed the pioneering work of Hess *et al.*,[20] and studied $NbSe_2$ by scanning tunneling microscopy (STM) and spectroscopy (STS). Observed systematic deviations of the SC DOS from the BCS form were attributed to the **k**-space anisotropy of the SC order parameter. However, the Fermi surface of the material has recently been explored in detail by Yokoya *et al.*[21] using high-resolution angle-resolved photoemission spectroscopy. The results suggest that the superconductivity in this material should be Fermi-surface sheet dependent. Moreover, other authors have inferred the existence of two gaps in $NbSe_2$, subject to a magnetic field, from thermal-conduction and heat-capacity measurements[22] wherein two corresponding coherence length scales ξ and ξ^* have been identified. However, $NbSe_2$ is *a priori* more complex than MgB_2 or V_3Si, having several bands crossing the Fermi level and manifesting competing charge-density wave order (see Refs. 21 and 23–27, and references therein). Its multiple-gap issue is not settled yet.

Importantly, the tunneling experiments were mostly realized in superconductor-insulator-normal-metal (SIN) geometry, only few superconductor-insulator-superconductor (SIS) data were reported.[28,29] In the latter case, a principal motivation was the high-energy resolution offered by SIS tunneling[30] as compared to the SIN case,[20,31] dominated by thermal smearing. Moreover, at very small tunneling resistances, Cooper pair tunneling across SIS junctions becomes possible, giving rise to a Josephson current.[32,33] This idea resulted in the discovery of the Josephson STM (JSTM) wherein the SC condensate is probed at the nanometer scale.[34,35]

However, the spectroscopy in the SIS configuration is still a challenge as it requires high-quality SC tips. Till now few SC tips have been developed for STM/STS: Pan *et al.*[28] and our group[34,36,37] reported STS with Nb tips while Rodrigo *et al.*[27,29,33] used Pb and Al tips. Yet other, more complex materials, such as MgB_2 can be used,[7] or even Ba_8Si_{46} clathrate tips (presented in this report, Sec. V). With such SC probes the fine variations in the SC DOS due to screening currents around a vortex in $NbSe_2$ were measured,[36] the vortices were probed with a very high spatial and energy resolution,[26,27,38] magnetic impurities at the surface of a SC sample were studied.[39] Thus, the use of SC STM/STS tips can potentially give more precise information about the DOS. This is of specific interest in the case of $NbSe_2$, for which both anisotropic gap and multiple gaps scenario were suggested.[26,27]

In this paper we generalize the idea of Schmidt *et al.*[14] and apply the Schopohl-Scharnberg-McMillan (SSM) model[40,41] to generate numerically the SC DOS of a two-band SC in the presence of a nonzero quasiparticle (QP) interband scattering in **k**-space (Sec. II). In Sec. III we discuss how this SC DOS appears in the tunneling spectroscopy data: both SIN and SIS geometries are considered. We demonstrate a very high sensitivity of the SIS tunneling to tiny deviations of the SC DOS from the BCS shape, *invisible in* SIN *data*, and predict their characteristic features. In Sec. IV we analyze in detail the SIS tunneling spectra considering an additional **k** selectivity of the *tunneling process* and discuss the contribution of each of two bands to the tunneling current. In particular, we show how a variety of spectral signatures (the "dips," "bumps," or "kinks") arises due to this **k** selection when the tunneling to the one of the two bands dominates the total tunneling spectrum. Importantly, we show that due to the interband quasiparticle coupling, even if only one band is probed (due to the tunneling selection reasons, for instance), the measured tunneling spectrum contains however all important information about the SC DOS in both bands, i.e., also about the DOS in the other, non-probed band. In Sec. V, we report a detailed SIS spectroscopy study of $NbSe_2$ using both Nb and Ba_8Si_{46} SC tips. We applied the modified SSM model (developed in Secs. II–IV) to fit the measured tunneling conductance spectra. To simplify the analysis, we considered isotropic SC gaps in each band, neglecting effects of anisotropy. Basing on very precise fits to the data, we infer the unique SC DOS of $NbSe_2$ which is strongly affected by the quasiparticle scattering between at least two different Fermi-surface sheets. We *postulate* that the *c*-axis SIS tunneling occurs preferentially to the electronic band where the leading (large) SC gap opens while a smaller (partially scattering-induced) SC gap exists in the other, non-probed band. Thus the situation is just opposite to the case of *c*-axis tunneling to MgB_2 where the main contribution to the current is to the π band revealing a small, induced gap.[42]

In general, physical phenomena involving mainly quasiparticles from one Fermi sheet, tied to either a small or a large gap within an intrinsically multigap SC, could be quite common. In $NbSe_2$ the second (smaller) gap was inferred from the specific-heat data[43] while it has not been directly observed in tunneling. Thus, our analysis may help to explain the discrepancies between the various types of experiments. It provides a method to detect the multigap superconductivity which could be applied to A15 compounds, Chevrel phases, borocarbides, pyrochlore SCs, and many others.

II. MULTIGAP SUPERCONDUCTIVITY

Fifty years ago Suhl *et al.*,[9] extended the one-band isotropic BCS model to the case where two energy bands cross the Fermi level and considered the possibility of phonon exchange between quasiparticles belonging to the two different bands. Such a two-band SC has two distinct gaps in its excitation spectrum, Δ_1 and Δ_2, which depend on the electron-phonon coupling in the corresponding bands 1 and 2, but also on the interband term reflecting the Cooper-pair tunneling. Analytically, the shape of the excitation spectrum $N^S(E)$ of such a two-gap SC is just the sum of two BCS spectra $N_i^S(E)$, $i=1,2$ with two different parameters Δ_i,

$$N^S(E) = \sum_{i=1,2} N_i^S(E) = \sum_{i=1,2} N_i(E_F) \frac{|E|}{\sqrt{E^2 - \Delta_i^2}}, \tag{1}$$

where $N_i(E_F)$ $i=1,2$ are partial normal-state DOS in the corresponding bands. The calculation can be extended to the case of an arbitrary number m of bands and the DOS is then a simple sum of m BCS terms. Later on Schopohl and Scharnberg[40] improved the Suhl model by including the quasiparticle scattering from one band to another. The model considers two interband scattering times τ_{12} and τ_{21} and results in two coupled equations for the gaps which become energy dependent $\Delta_i \rightarrow \Delta_i(E)$. Formally, these equations are identical to those developed by McMillan[41] for the proximity effect. The underlying mechanism is indeed a "proximity effect" but in reciprocal space, the quasiparticles of the SC condensate in one energy band scatter to a second band and vice versa, thus modifying the total excitation spectrum,

$$\Delta_1(E) = \frac{\Delta_1^0 + \Gamma_{12}\Delta_2(E)/\sqrt{\Delta_2^2(E) - (E - i\Gamma_{21})^2}}{1 + \Gamma_{12}/\sqrt{\Delta_2^2(E) - (E - i\Gamma_{21})^2}}, \tag{2a}$$

$$\Delta_2(E) = \frac{\Delta_2^0 + \Gamma_{21}\Delta_1(E)/\sqrt{\Delta_1^2(E) - (E - i\Gamma_{12})^2}}{1 + \Gamma_{21}/\sqrt{\Delta_1^2(E) - (E - i\Gamma_{12})^2}}, \tag{2b}$$

where Δ_i^0 are intrinsic SC gaps in each band, and the scattering frequencies Γ_{12} and Γ_{21} are nothing but inverse of Schopohl-Scharnberg scattering times τ_{12} and τ_{21}. In addition, Γ_{ij} should fulfill, $\Gamma_{12}/\Gamma_{21} = N_2(E_F)/N_1(E_F)$. This condition reflects the fact that the interband scattering events in **k** space $1 \rightarrow 2$ and $2 \rightarrow 1$ should be equal.[40] For each band ($i=1,2$), the gap $\Delta_i(E)$ in Eq. (2) depends on the intrinsic gap Δ_i^0 plus a term induced by the second band via quasiparticle scattering. The excitation spectrum of such a SC is in each band,

$$N_i^S(E) = N_i(E_F)\mathrm{Re}\left\{\frac{|E|}{\sqrt{E^2 - \Delta_i(E)^2}}\right\}. \tag{3}$$

The total SC of the material is then a sum of partial SC DOSs, as in Eq. (1).

In principle, the Eq. (2) could be extended to the anisotropic case, i.e., $\Delta_i = \Delta_i(\mathbf{k})$ and $\Gamma_{ij} = \Gamma_{ij}(\mathbf{k}, \mathbf{k}')$, which is there-

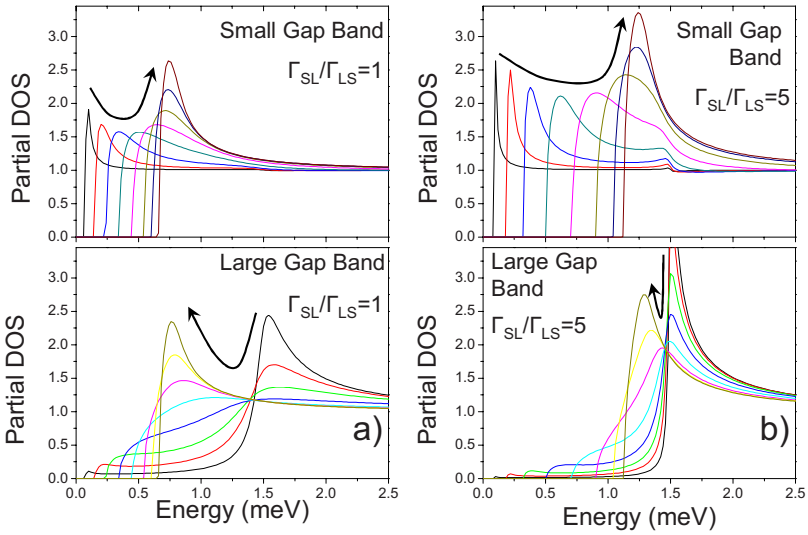

FIG. 1. (Color online) Calculated partial DOSs at $T=0$ for the bands S and L. The intrinsic gap in the band S is $\Delta_S^0=0$ meV, and the one in the band L is $\Delta_L^{ph}=1.5$ meV. In (a) result for the ratio $\Gamma_{SL}/\Gamma_{LS}=1$. In (b) result for $\Gamma_{SL}/\Gamma_{LS}=5$. Different curves correspond to $\Gamma_{SL}=(0.1,0.25,0.5,1,2,4,8,16)$. At low coupling Γ_{ij} a large superconducting gap exists in the band L, the gap in the band S being much smaller. With increasing the coupling, the gap in the band L progressively decreases and that in the band S increases. The corresponding movement of states is shown by arrows. At the limit of very high Γ_{ij} the DOS in both bands coincide, characterized by one single gap of a width depending on the Γ_{SL}/Γ_{LS} ratio.

fore fully **k** dependent and equivalent to existing, more sophisticated, theories.[15–17,44] The full approach necessarily increases the number of parameters to consider. Here, in our simplified model we neglect the anisotropy of initial SC gaps and consider two bands: the band $S(i=1)$ to have a smaller constant initial gap $\Delta_1^0(\mathbf{k})=\Delta_S^0$ and the band $L(i=2)$ to have a larger constant initial gap $\Delta_2^0(\mathbf{k})=\Delta_L^0$. We also neglect the **k** anisotropy of scattering rates, $\Gamma_{12}(\mathbf{k})=\Gamma_{SL}$ and $\Gamma_{21}(\mathbf{k})=\Gamma_{LS}$. We thus have a set of four parameters (i.e., Δ_S^0, Δ_L^0, Γ_{LS}, and Γ_{SL}) which decide the partial DOSs in the bands S and L. One should not forget that physically, the parameters Γ_{SL} and Γ_{LS} are linked via the ratio $N_L(E_F)/N_S(E_F)$ of the partial normal-state DOS in each band.[40] Thus, only three parameters remain indeed independent in our model.

In Fig. 1 we give an example of the numerically generated partial SC DOS (bands L and S) of such a two-band SC. For this illustration we have chosen the extreme case when $\Delta_S^0=0$, i.e., the gap in the band S is fully induced via the interband quasiparticle coupling to the band L, where $\Delta_L^0=1.5$ meV. Figure 1(a) shows the case where two bands have equal normal-state densities, $N_L(E_F)=N_S(E_F)$, $\Gamma_{SL}/\Gamma_{LS}=1$. In Fig. 1(b) we show a more realistic case where the large gap band L is characterized by a higher normal-state DOS, $N_L(E_F)=5N_S(E_F)$, and consequently, $\Gamma_{SL}/\Gamma_{LS}=5$. It is clear from Fig. 1 that the shape of the partial DOS in each band strongly deviates from the noncoupled BCS case and depends significantly on the strength of the interband coupling. The latter increases with the density of scatterers in a given sample but may also exist in a pure sample due to electron-electron interactions.

III. SIS VERSUS SIN TUNNELING SPECTROSCOPY

Tunneling spectroscopy in planar junctions as well as in STM experiments is an important probe of the DOS of materials. In the STM geometry, the current across the STM junction is a convolution of the DOS of the STM tip $N_{tip}(E)$, that of the studied sample $N_{sample}(E)$, and the Fermi-Dirac function $f(E)$,

$$I(V) = I_0 \exp(-2\alpha_k z) \times \int_E N_{tip}(E) N_{sample}(E+eV) \times [f(E) - f(E+eV)]dE. \quad (4)$$

The presence of the Fermi-Dirac functions in the Eq. (4) limits the energy resolution of a standard SIN measurement [normal-metal tip, $N_{tip}(E) \simeq cte$] to $\sim 3.5kT$. This thermal smearing often prevents the observation of weak features in the DOS.[45] Two DOS features separated by an energy interval on the order of $3kT$ (or less than ~ 0.2 meV at 2.5 K) will remain unresolved by standard SIN spectroscopy.

An entirely different approach to overcome thermal broadening problems in the tunneling spectroscopy is to use superconducting STM tips. Indeed, the peculiar sharp-peaked DOS of the SC tip may considerably enhance the spectroscopic resolution, which is clearly understood from the convolution integral, Eq. (4). The effect of the SIS resolution enhancement is illustrated by the simulation in Fig. 2(a), where we consider the BCS DOS (black line) and the associated tunneling conductance at $T=2.5$ K in SIN [red (dark gray) line] as well as in SIS geometry [green (light gray) line]. Note how the thermal smearing drastically smooths the SIN spectrum, while in contrast, the SIS mode gives very sharp peaks.[30] It is important to stress that, for two SC electrodes with BCS DOS, the SIS conductance looks like a gap delimited by two very sharp deltalike quasiparticle peaks, followed by a constant background. Hence, any departure from this very specific shape due to a non-

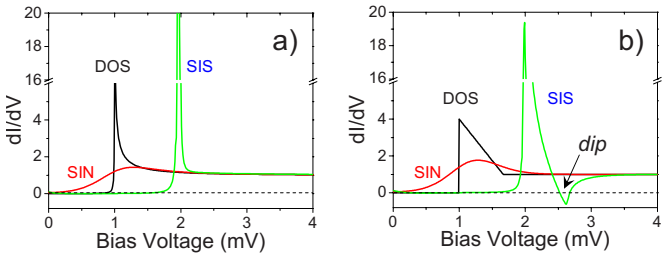

FIG. 2. (Color online) In (a) BCS DOS with $\Delta=1.0$ meV (black line), the corresponding SIN [red (dark gray) line] and SIS [green (light gray) line] tunneling conductance at $T=2.5$ K. For the SIS case two identical BCS DOS electrodes were considered. In (b) non-BCS DOS with triangular peaks (black line), and the corresponding SIN [red (dark gray)] and SIS [green (light gray)] tunneling conductance at $T=2.5$ K. For this SIS case the BCS DOS with $\Delta=1.0$ meV was considered for the second SC electrode. Note how the departure from the BCS DOS results in damped and enlarged peaks but also in appearance of a dip that may even take a negative value. SIN spectra remain smooth and featureless in both cases.

BCS DOS of one of the electrodes forming the SIS junction should be easily detected.

A simple but clear example of such sensitivity is provided in Fig. 2(b) where we have chosen a simple but nonrealistic SC DOS with triangular quasiparticle peaks (black solid line). Remarkably, the simulation of the SIS [green (light gray) line] tunneling spectra (the SC DOS of the second electrode is taken of BCS-type) results in well-pronounced dips with a low (or even negative) tunneling conductance. Note that the corresponding SIN conductance spectrum [red (dark gray) line in Fig. 2(b)] remains almost insensitive to this SC DOS modification.

IV. SIS TUNNELING TO A TWO-GAP SUPERCONDUCTOR

In this section we consider the SIS tunneling in the case when at least one of the electrodes is a two-gap SC with two (or more) energy bands at the Fermi level. We show how the different spectroscopic signatures arising in the SIS spectra depend on the **k** selectivity of the tunneling process. Note, that the widely used expression for the tunneling current [Eq. (4)] does not take into account the **k** selectivity. However, even in the lowest order, the tunneling conductance, such as in the Tersoff and Hamann theory,[46] is proportional to a **k**-dependent transmission coefficient (see Ref. 47 for a more complete discussion),

$$T_{\mathbf{k}}(z) \simeq |c_{\mathbf{k}}|^2 \exp(-2\alpha_k z). \tag{5}$$

Here $c_{\mathbf{k}}$ is the amplitude of the surface wave function, z is the barrier width, and α_k^{-1} is the attenuation length in vacuum. In fact, the latter is such that

$$\alpha_k = \sqrt{k_\parallel^2 + 2m\varphi/\hbar^2}, \tag{6}$$

where $k_\parallel$ is the surface wave vector and φ is the work function. Here, one assumes a simple Fermi surface, so the expressions (5) and (6) represent the tunneling "cone" wherein the tunneling conductance dI/dV is due to states with small $k_\parallel$, or near the *surface* Brillouin-zone center ($k_\parallel=0$). In such a case, one could take $\alpha_k \simeq (2m\varphi/\hbar^2)^{1/2}=\kappa$, equivalent to tunneling along the z axis. Thus, in the simple case of a spherical Fermi surface, this approximation suffices, the explicit **k** dependence of $T_{\mathbf{k}}(z)$ may be replaced by an effective **k**-averaged value leading to Eq. (4).

For more complex Fermi-surface sheets, such as in layered materials, with Fermi cylinders parallel to the c axis, some care must be taken since there may be no states at all for $k_\parallel \simeq 0$, and clearly, the tunneling spectrum would not correspond exactly to the full **k**-averaged density of states, as implied by our Eq. (4). This situation is encountered specifically in the multiband SC, in which the electrons tunnel to different Fermi-surface sheets.

The exact tunneling conductance is a sum over the partial DOS of a quasiparticle of momentum **k** times the probability $T_{\mathbf{k}}(z)$, defined by Eq. (5). We already presented this approach, based on the theory of Tersoff and Hamann,[46] in the context of CaC_6.[47]

For the present work, such a full (and complex) description of the tunneling conductance turns out to be unnecessary. In the spirit of Eq. (4), wherein a single effective tunneling current is defined, we develop a heuristic approach to the measured tunneling DOS in the case of two or more bands. We suggest that, instead of doing summation over all **k**, one can average first over the **k**-dependent transmission for each band *separately*, and then, to calculate the total tunneling current as a sum of partial terms arising from each band. Using this idea and Eq. (3), we write the total *tunneling* DOS as

$$N^S_{tunnel}(E) \propto \sum_i T_i^{eff} N_i(E_F) \mathrm{Re}\left\{ \frac{|E|}{\sqrt{E^2-\Delta_i^2}} \right\}, \tag{7}$$

where T_i^{eff} represents the fraction of the *transmitted* tunneling electrons arriving to (or from) the ith band; it thus fulfills $\Sigma T_i^{eff}=1$. The total tunneling current is obtained using Eq. (4) in which one should replace $N_{sample}(E)$ by $N^S_{tunnel}(E)$. As we will see in Sec. V, this approach turns out to give an excellent fit to the experimental data.

In order to illustrate the above idea let us consider the well-studied case of MgB_2. In this material there are two different bands of different character: the two-dimensional σ band, with a gap of 7.2 meV, and the three-dimensional (3D) π band, with a smaller (partially induced) gap of 2.5 meV. Tunneling spectroscopy along the c axis measures the small gap because the cylindrical sheet of the σ band (large $k_\parallel$) is not as favorable as the 3D locally spherical sheet of the π band (small $k_\parallel$). Obviously, one can measure the anisotropy by tunneling in different directions.[42] It is important in our approach that it should be possible to detect the multigap signatures even if the tunneling occurs to only one of two electronic bands. Indeed, SIS c-axis tunneling spectra of MgB_2 showed characteristic dips which are a consequence of the two-gap SC of this material.[14] This is directly corroborated by our Fig. 1(b) and Eq. (7) making an appropriate choice of T_S^{eff} (π band) and T_L^{eff} (σ band), $T_L^{eff} \ll T_S^{eff}$, as expected.

Although MgB_2 is quite extreme, the effects of **k** selectivity are more common than previously thought. It is also

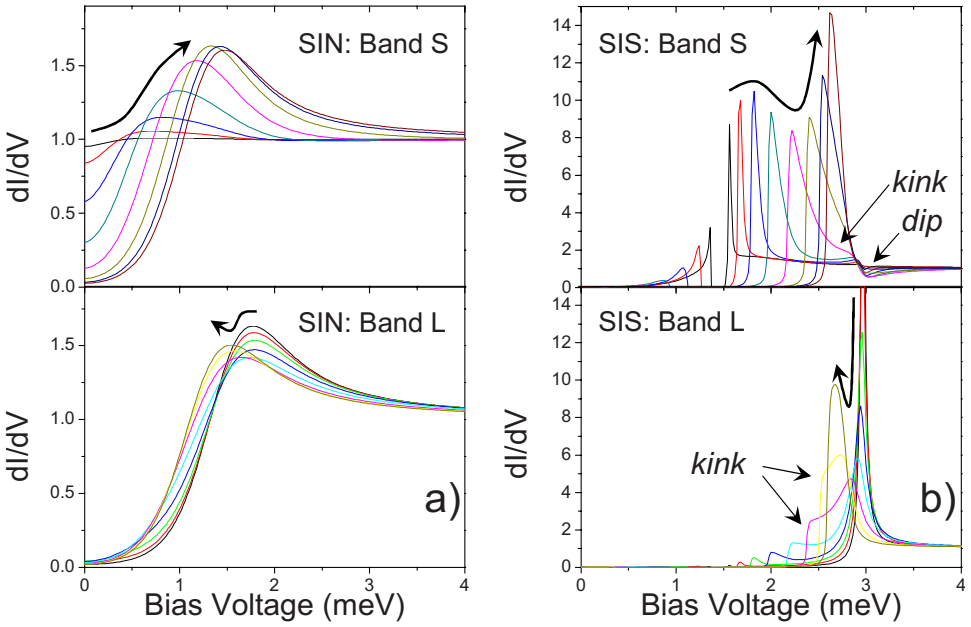

FIG. 3. (Color online) Calculated partial tunneling conductance spectra at $T=2.5$ K for the bands S and L. The considered Δ_i^0 and Γ_{ij} parameters are the same as in Fig. 1(b), $\Gamma_{SL}/\Gamma_{LS}=5$. In (a) partial SIN tunneling spectra are featureless. In (b) partial SIS tunneling spectra show sharp peaks, characteristic kinks and dips. The evolution of the spectra with increasing the quasiparticle interband coupling is shown by arrows.

illustrated by the recent SC compound CaC_6. Evidence for the anisotropy of this material was given by Gonnelli *et al.*[48] who showed that point-contact spectroscopy in different directions led to different gap values. This effect was difficult to detect from our SIN tunneling measurements parallel to the c axis.[47] In this instance, the small deviation from standard one-band BCS could be interpreted either as a weak Γ_{Dynes} (Ref. 49) or a small anisotropy, and a definite conclusion could not be given. In view of Eq. (4), it is probable that an SC tip would have been sensitive enough to detect the anisotropy, even at $T=2.5$ K. In summary, the largest effect on the spectrum is still the multigap superconductivity with interband coupling, well described by the heuristic model [Eq. (7)], and further supported by the SIS measurements presented below.

In Fig. 3 we calculate the partial contributions to the tunneling conductance of each of two bands (S,L) of our hypothetic two-band SC using the calculated partial SC DOS, Fig. 1(b). The conductance in both SIN and SIS configurations are displayed, where the counterelectrode is, respectively, a normal-metal [Fig. 3(a)] or a conventional SC with a constant BCS gap of 1.5 meV [Fig. 3(b)]. As discussed in Sec. III, the SIN spectra appear smooth and featureless for both SC bands while their SIS counterparts show a well-developed "pathological" shape. The partial SIS tunneling conductance in the band S shows sharp gap edges followed by kinks and dips at higher energy [Fig. 3(b), upper panel], whereas the SIS tunneling to the band L leads to spectra characterized by kinks inside the quasiparticle peaks [Fig. 3(b), lower panel]. In order to evaluate the total SIS tunneling conductance spectra, these partial SIS contributions should be added with their respective tunneling weights T_i^{eff}, as it was done above for the partial DOS, Eq. (7). In practice, when the tunneling process selects mainly the small gap band S, dips will be visible in SIS spectra outside the gap. Their amplitude increases with the coupling between the bands Γ_{21}. In the opposite situation, when the tunneling takes place mainly toward the large-gap band L, the kinks inside the gap will be visible in the SIS spectra. As expected, none of these features are detectable in the SIN conductance spectra at $T=2.5$ K because of the thermal smearing [Fig. 3(a)]. We note that the dips may arise neither from the gap anisotropy nor from any model wherein the DOS is expressed as a weighted sum of BCS DOS. We have studied numerically such cases and the dips we have illustrated in Fig. 3(b) appeared in the SIS spectra only for a strong enough interband coupling. We should remind however, that due to the formal equivalency between the interband coupling in **k** space[40] and the proximity effect in the real space,[41] the dips may also appear in the case of a proximity layer formed at the surface of the probed SC, even if the latter has only one SC gap in the bulk.[50] The kinks inside the gap [Fig. 3(b)] cannot appear in such a case since they may arise only in the DOS of the SC material.

V. SIS TUNNELING STUDY OF $NbSe_2$

The deviation of the SC DOS in $NbSe_2$ from the conventional BCS shape was reported already 20 years ago by Hess *et al.*[20] who observed SIN tunneling spectra with broadened peaks and unusual bumps inside the SC gap. For a long time these deviations were interpreted as due to the angular **k**-space anisotropy of the order parameter. However, other experimental data[21,22,43,51,52] were analyzed considering the SC DOS with two distinct BCS terms (i.e., with only two constant SC gaps), *in fine* equivalent to Suhl's two-gap model, Eq. (1).[53] Indeed, the Fermi surface of $NbSe_2$ contains two sets of multiwalled cylinders: one set is centered at K points of the hexagonal Brillouin zone and the other around the central Γ point. Such a complex Fermi surface may lead, in principle, to a multisheet superconductivity with two (or more) SC gaps. Huang *et al.*[43] studied temperature and magnetic field dependence of the specific heat and deduced $\Delta_1=0.73$ meV and $\Delta_2=1.26$ meV. Ying *et al.*[51] found $\Delta_1=0.85$ meV and $\Delta_2=1.5$ meV from their specific-heat measurements. The penetration depth measurements by

Fletcher *et al.*[52] gave $\Delta_1=0.66$ meV and $\Delta_2=1$ meV. By measuring the magnetic field dependence of the thermal conductivity and that of the specific heat, Boaknin *et al.*[22] identified two characteristic magnetic fields values H_{c2} (critical magnetic field) and H^*. They found $H^*=H_{c2}/9$. From this field values they calculated two characteristic length scales, ξ and ξ^*, using $\xi=\sqrt{\Phi_0/2\pi H}$ that they explained in terms of multigap superconductivity with the ratio $\Delta/\Delta^*\sim 3$ between the large and small gap.[54] Remarkably, the authors of most of the above cited reports pointed out that they were unable to distinguish between a two-gap model and a continuously varying anisotropic gap.

In the search for a higher-energy resolution (see Sec. III of the present paper) some groups have studied $NbSe_2$ by STS in the SIS regime using SC tips of Pb (Refs. 27 and 29) or Nb.[28,36,37] Rodrigo *et al.*[27,29] reached probably the best spectroscopic resolution and deduced the total tunneling DOS of $NbSe_2$ as it comes from the *c*-axis SIS tunneling. The observed tunneling DOS was approximated by a sum of BCS-type DOSs with an inferred continuous gap distribution. The analysis resulted in a very broad gap distribution characterized by two distinguishable plateaus centered at 0.7 and 1.3 meV. According to the authors, these two plateaus are the signature of a two-band SC, in the spirit of Suhl *et al.*,[9] i.e., no interband coupling being considered, each band being characterized by strongly anisotropic gap distribution (related to the charge-density wave). The **k** selectivity of the tunneling process was not considered and each point of the Fermi surface was believed to contribute equally to the tunneling current.

We measured SIS conductance spectra of $NbSe_2$ using Nb as well as Ba_8Si_{46} tips. The Nb tips were prepared by breaking a fine high-purity niobium wire in ultrahigh vacuum.[37] The Ba_8Si_{46} clathrate tips were achieved by first gluing a small grain of the material on a PtIr tip, then cleaving them *in situ* to obtain a fresh noncontaminated surface. The characteristic tunneling spectra are presented in Fig. 4(a) (Ba_8Si_{46} tips) and in Fig. 4(b) (Nb tips). At first glance, the experimental results obtained with various SC tips seem quite similar but a closer inspection reveals net differences depending on the precise nature of the STM tip. Specifically, when using Nb tips, small dips are visible in some selected spectra while they are absent in others. On the other hand, small but clear dips are always observed when Ba_8Si_{46} tips are used. The dips are absent in Pb-$NbSe_2$ SIS tunneling data.[27,29]

These slight differences may simply be explained by the presence of a proximity layer at the tip surface or by a two-gap superconductivity in the tip material.[55] We have checked numerically that once the tunneling DOS of the tip is properly accounted for, the inferred total tunneling SC DOS of $NbSe_2$ appeared quite the same for all studied junctions. It clearly agrees with that observed by Hess *et al.*[20] and improved by Rodrigo *et al.*[27,29] It is characterized by broadened peaks with "kinks" inside the gap.

While the shape of the total tunneling DOS of $NbSe_2$ is now well established, we propose a radically different interpretation of the observed signatures. Instead of considering independent two-band superconductivity with a complicated distribution of the SC gaps over each band, we apply the interband coupling model described in Sec. II, together with

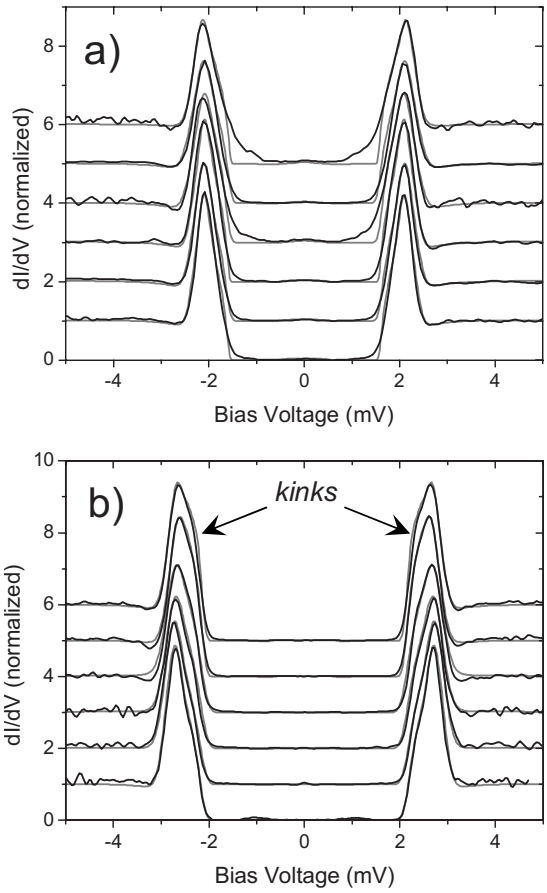

FIG. 4. SIS tunneling spectra measured at $T=2.5$ K at different locations and on various samples of $NbSe_2$. In (a) using Ba_8Si_{46} STM tips and in (b) using Nb tips. In all cases the tunneling resistance was $R_T=13$ MΩ. The spectra are shifted for clarity. Note the enlarged asymmetric peaks and characteristic kinks inside the apparent gap, clearly seen. Thin gray lines: the fits by SSM model using the parameters shown in Fig. 5.

the **k**-selection considerations, Sec. IV First of all, we neglect the anisotropy of the intrinsic gaps in each band (as we show below, there is simply no need for it) and thus, only two-gap parameters remain, Δ_S^0, Δ_L^0. The interband coupling is taken into account by Γ_{SL} and Γ_{LS} (linked together through Schopohl-Scharnberg condition, Sec. II). Within SSM model these parameters fully define the partial SC DOS in each band (Sec. II). The knowledge of partial DOSs is however not enough to calculate the tunneling spectra. Indeed, due to the **k** selectivity of the STM, in particular, for tunneling along the *c* axis of a layered material, different sheets of the Fermi surface do not participate equally to the tunneling. We believe that our Eq. (7) is a reasonable approximation for describing the effect of two-sheet SC for the *tunneling* DOS. Thus, in order to account for the total tunneling signal, we need one more free parameter, T_S^{eff}, reflecting the efficiency of the tunneling process toward the band *S* (T_L^{eff} simply fulfills $T_L^{eff}=1-T_S^{eff}$, in our two-band tunneling model).

The results of the fits to the experimental SIS data are presented as thin solid lines in Fig. 4. It is amazing how nicely the numerically generated curves reproduce the characteristics of the tunneling spectra. But what is indeed re-

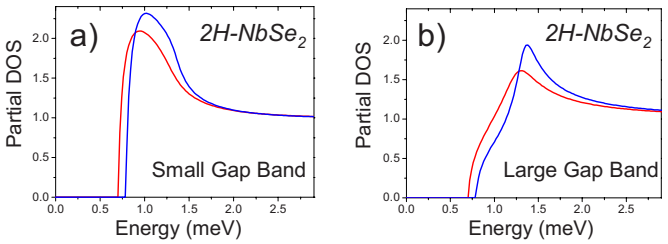

FIG. 5. (Color online) The partial DOS calculated in the framework of SSM approach for two SC bands of 2H-$NbSe_2$ that give the best fits of the SIS tunneling spectra in Fig. 4 and the data Ref. 27. In red (gray), the fits with $\Gamma_{SL}/\Gamma_{LS}=3$ and in blue (black), the fits with $\Gamma_{SL}/\Gamma_{LS}=5$. In both cases $\Delta_L^0=1.41$ meV, $\Delta_S^0=0$ meV, and $\Gamma_{SL}=3$ meV.

markable are the values of the fitting parameters for the tunneling DOS of $NbSe_2$ that we obtained for *all* studied spectra. First, we found that $T_S^{eff}\simeq 0$, i.e., the tunneling occurs essentially to the large gap band $L(T_L^{eff}\simeq 1)$, the band (S) being not probed in the c-axis tunneling experiment. Second, the best result is obtained putting $\Delta_S^0=0$, meaning that there is no intrinsic superconductivity in the band S, and the gap in the partial DOS $N_S^S(E)$ arises only due to the interband scattering coupling to the band L where a large intrinsic SC gap exists $\Delta_L^0=1.4\pm 0.1$ meV. Third, the parameters Γ_{SL} and Γ_{LS} vary from one spectrum to another but their ratio Γ_{SL}/Γ_{LS} takes in most cases one of two values: 3.5 or 5.0 (only in few local tunneling spectra the ratio was found to be between these two values). It is important to note that for the two different kinds of tips, Nb and Ba_8Si_{46}, we have obtained the same sets of parameters for $NbSe_2$ electrode. Thus, we suggest that, within SSM model, the c-axis tunneling measurements probe the energy band where the largest of two gaps exists. A clue for this is the large value of $2\Delta_L^0/kT_c\approx 4.18$ which is larger than the BCS ratio 3.52, as for strong electron-phonon coupling. While the small (induced) gap is not directly observed (since the corresponding electronic band is not probed in this tunneling configuration, $T_S^{eff}\simeq 0$) it is indeed responsible for the kinks experimentally observed inside the quasiparticle peaks, as predicted by SSM model [Fig. 1(b)].

Another important issue is the found constant ratio Γ_{SL}/Γ_{LS}, 3.5 or 5.0. In the framework of our model, this value corresponds to the ratio of partial normal-state densities of two bands (Schopohl-Scharnberg condition, Sec. II). We *speculate* that the two inferred values correspond to the presence (or absence) in the locally probed region of $NbSe_2$ of the charge-density waves—a collective effect that suppresses some electronic states from the Fermi surface due to the partial nesting. This issue should be fixed in the future experiments.

Finally, basing on the high quality of the fits obtained with only two really free parameters, Δ_L^0 and Γ_{SL}, we extracted the partial DOSs for two Fermi sheets involved in the superconductivity of $NbSe_2$; they are plotted in Fig. 5. For the leading SC band L, the large gap opens characterized by nondiverging broadened quasiparticle peaks at 1.3–1.5 meV and kinks inside the gap. For the band S, where the superconductivity is induced, the DOS is characterized by damped and enlarged quasiparticle peaks with the maxima at 0.9–1.0 meV followed by kinks at higher energy. The full (excitation) gap opens in both bands only at 0.65–0.8 meV. These characteristic energies are revealed experimentally. They are indeed in good agreement with those reported in previous measurements[43,51,52] (see the gap values reported at the beginning of this section, see also Ref. 54). We must remind here, that our interpretation is based on QP interband scattering effect, it is thus very different from the pair scattering Suhl's model, Eq. (1), used in the above cited papers.

The partial DOSs in Fig. 5 have pathologically non-BCS shape. We used it to fit other available tunneling SIS data measured on both $NbSe_2$ (Ref. 27) and NbS_2.[56] We found that, in both materials, the total SC DOS may be described by two SSM partial DOSs, taking for $NbSe_2$: $\Delta_L^0=1.43$ meV, $\Gamma_{SL}=3.36$ meV, $\Gamma_{SL}/\Gamma_{LS}=3.0$, and for NbS_2: $\Delta_L^0=1.15$ meV, $\Gamma_{SL}=1.5$ meV and $\Gamma_{SL}/\Gamma_{LS}=3.8$. The reported SIS tunneling conductance data[27,56] are then fitted with excellent accuracy. The essential difference we found between two cases is that in the case of NbS_2 the required tunneling transmission fractions are $T_L^{eff}=0.55$ and $T_S^{eff}=0.45$ while they are found, respectively, 1 and 0 in the case of $NbSe_2$. Thus, unlike the case of 2H-$NbSe_2$ where only the band L effectively contributes to the tunneling current, the c-axis tunneling toward NbS_2 occurs with significant contribution of both SC bands.

VI. CONCLUSION

In conclusion, numerous reported tunneling data measured on "conventional" superconductors ($NbSe_2$, MgB_2, CaC_6, etc.) show significant deviations from the BCS form. These deviations cannot be easily accounted for in the framework of multiple-gap models of Suhl' type[9] that lead to the weighted sum of standard BCS DOS. We started with the model of Schopohl-Scharnberg for two-band superconductivity in the presence of quasiparticle interband scattering, and we developed it to the case of **k**-selective tunneling, obvious in the case of complex multisheet Fermi-surface materials. The Schopohl-Scharnberg model predicts characteristic features—kinks, dips, damped quasiparticle peaks—to appear in the partial DOS due to the scattering of quasiparticles. We noted that, due to the formal equivalency between Schopohl-Scharnberg formalism and McMillan approach for real-space proximity effect, the two effects may be easily confused and thus, a deeper analysis is required. We applied the developed SSM model to the case of 2H-$NbSe_2$ for which the tunneling spectrum has been established in finer detail due to the enhanced resolution offered by SIS geometry. In the framework of developed SSM model we succeeded to fit the experimental data with very high fidelity, using only three free parameters having each very clear physical meaning. Our result suggests that the case of $NbSe_2$ is very similar to that of MgB_2, for which the SSM approach has already been successfully applied,[14] i.e., $NbSe_2$ is a multiple-band superconductor in which the SC gap in one (driven) band is induced by interband scattering of quasiparticles from the another (leading) one. The main difference between MgB_2 and $NbSe_2$ is then in the tunneling process:

the *c*-axis tunneling to MgB_2 occurs mainly to 3D π band revealing the smaller gap in the tunneling spectra, whereas in the case of $NbSe_2$ the leading SC band with the larger gap is probed. The latter fact allows us to exclude the hypothesis of the proximity layer at the surface of $NbSe_2$ which was plausible for MgB_2.[7] Further study is needed to probe directly the band with the smaller (induced) gap in $NbSe_2$. In fact, structural defects, voids, and atomic steps at the surface of the material may locally modify the tunneling selection rules, thus favoring the tunneling process toward another, usually nonprobed band. Such a STM/STS experiment could decide the issue of multiple-band superconductivity in this material.

ACKNOWLEDGMENTS

The authors wish to thank V. Dubost (INSP, Paris, France) for relevant remarks concerning the manuscript, J. F. Zasadzinski (Physics Department, Illinois Institute of Technology, USA) and R. Chitra (LPTL, University of Paris 6, France) for interesting discussions.

[1] J. Bardeen, L. N. Cooper, and J. R. Schrieffer, Phys. Rev. **108**, 1175 (1957).
[2] D. J. Van Harlingen, Rev. Mod. Phys. **67**, 515 (1995), and references therein.
[3] I. Giaever, H. R. Hart, Jr., and K. Megerle, Phys. Rev. **126**, 941 (1962).
[4] D. J. Scalapino, J. R. Schrieffer, and J. W. Wilkins, Phys. Rev. **148**, 263 (1966).
[5] J. Nagamatsu, N. Nakagawa, T. Muranaka, Y. Zenitani, and J. Akimitsu, Nature (London) **410**, 63 (2001).
[6] F. Bouquet, Y. Wang, R. A. Fisher, D. G. Hinks, J. D. Jorgensen, A. Junod, and N. E. Phillips, Europhys. Lett. **56**, 856 (2001).
[7] F. Giubileo, D. Roditchev, W. Sacks, R. Lamy, D. X. Thanh, J. Klein, S. Miraglia, D. Fruchart, J. Marcus, and P. Monod, Phys. Rev. Lett. **87**, 177008 (2001).
[8] P. Szabó, P. Samuely, J. Kačmarčík, T. Klein, J. Marcus, D. Fruchart, S. Miraglia, C. Marcenat, and A. G. M. Jansen, Phys. Rev. Lett. **87**, 137005 (2001).
[9] H. Suhl, B. T. Matthias, and L. R. Walker, Phys. Rev. Lett. **3**, 552 (1959).
[10] J. C. F. Brock, Solid State Commun. **7**, 1789 (1969).
[11] L. Y. L. Shen, N. M. Senozan, and N. E. Phillips, Phys. Rev. Lett. **14**, 1025 (1965).
[12] M. R. Eskildsen, M. Kugler, S. Tanaka, J. Jun, S. M. Kazakov, J. Karpinski, and Ø. Fischer, Phys. Rev. Lett. **89**, 187003 (2002).
[13] M. Iavarone, G. Karapetrov, A. E. Koshelev, W. K. Kwok, G. W. Crabtree, D. G. Hinks, W. N. Kang, E.-M. Choi, H. J. Kim, H.-J. Kim, and S. I. Lee, Phys. Rev. Lett. **89**, 187002 (2002).
[14] H. Schmidt, J. F. Zasadzinski, K. E. Gray, and D. G. Hinks, Physica C **385**, 221 (2003).
[15] A. Y. Liu, I. I. Mazin, and J. Kortus, Phys. Rev. Lett. **87**, 087005 (2001); Y. A. Liu and I. I. Mazin, Phys. Rev. B **75**, 064510 (2007).
[16] H. J. Choi, D. Roundy, H. Sun, M. L. Cohen, and S. G. Louie, Phys. Rev. B **66**, 020513(R) (2002).
[17] J. Kortus, O. V. Dolgov, R. K. Kremer, and A. A. Golubov, Phys. Rev. Lett. **94**, 027002 (2005).
[18] G. Wexler and A. M. Woolley, J. Phys. C **9**, 1185 (1976).
[19] J. A. Wilson, Phys. Rev. B **15**, 5748 (1977).
[20] H. F. Hess, R. B. Robinson, and J. V. Waszczak, Phys. Rev. Lett. **64**, 2711 (1990).
[21] T. Yokoya, T. Kiss, A. Chainani, S. Shin, M. Nohara, and H. Takagi, Science **294**, 2518 (2001).
[22] E. Boaknin, M. A. Tanatar, J. Paglione, D. Hawthorn, F. Ronning, R. W. Hill, M. Sutherland, L. Taillefer, J. Sonier, S. M. Hayden, and J. W. Brill, Phys. Rev. Lett. **90**, 117003 (2003); E. Boaknin, M. A. Tanatar, J. Paglione, D. G. Hawthorn, R. W. Hill, F. Ronning, M. Sutherland, L. Taillefer, J. Sonier, S. M. Hayden, and J. W. Brill, Physica C **408-410**, 727 (2004).
[23] W. Sacks, D. Roditchev, and K. P. Jean, Phys. Rev. B **57**, 13118 (1998).
[24] T. Valla, A. V. Fedorov, P. D. Johnson, P.-A. Glans, C. McGuinness, K. E. Smith, E. Y. Andrei, and H. Berger, Phys. Rev. Lett. **92**, 086401 (2004).
[25] K. Rossnagel, O. Seifarth, L. Kipp, M. Skibowski, D. Voß, P. Krüger, A. Mazur, and J. Pollmann, Phys. Rev. B **64**, 235119 (2001).
[26] I. Guillamon, H. Suderow, F. Guinea, and S. Vieira, Phys. Rev. B **77**, 134505 (2008).
[27] J. G. Rodrigo and S. Vieira, Physica C **404**, 306 (2004).
[28] S. H. Pan, E. W. Hudson, and J. C. Davis, Appl. Phys. Lett. **73**, 2992 (1998).
[29] H. Suderow, M. Crespo, P. Martinez-Sampera, J. G. Rodrigo, G. Rubio-Bollinger, S. Vieira, N. Luchier, J. P. Brison, and P. C. Canfield, Physica C **369**, 106 (2002).
[30] I. Giaever, Phys. Rev. Lett. **5**, 464 (1960); I. Giaever and K. Megerle, Phys. Rev. **122**, 1101 (1961).
[31] A. Yazdani, B. A. Jones, C. P. Lutz, M. F. Crommie, and D. M. Eigler, Science **275**, 1767 (1997).
[32] O. Naaman, W. Teizer, and R. C. Dynes, Phys. Rev. Lett. **87**, 097004 (2001); O. Naaman, R. C. Dynes, and E. Bucher, Int. J. Mod. Phys. B **17**, 3569 (2003).
[33] J. G. Rodrigo, H. Suderow, and S. Vieira, Eur. Phys. J. B **40**, 483 (2004).
[34] Th. Proslier, A. Kohen, Y. Noat, T. Cren, D. Roditchev, and W. Sacks, Europhys. Lett. **73**, 962 (2006). In this work Josephson (JSTM) mapping is done in the fluctuation regime.
[35] N. Bergeal, Y. Noat, T. Cren, Th. Proslier, V. Dubost, F. Debontridder, A. Zimmers, D. Roditchev, W. Sacks, and J. Marcus, Phys. Rev. B **78**, 140507(R) (2008).
[36] A. Kohen, Th. Proslier, T. Cren, Y. Noat, W. Sacks, H. Berger, and D. Roditchev, Phys. Rev. Lett. **97**, 027001 (2006).
[37] A. Kohen, Y. Noat, T. Proslier, E. Lacaze, M. Aprili, W. Sacks, and D. Roditchev, Physica C **419**, 18 (2005).
[38] J. G. Rodrigo, V. Crespo, and S. Vieira, Physica C **437-438**, 270 (2006).
[39] S.-H. Ji, T. Zhang, Y.-S. Fu, X. Chen, X.-C. Ma, J. Li, W.-H. Duan, J.-F. Jia, and Q.-K. Xue, Phys. Rev. Lett. **100**, 226801 (2008).
[40] N. Schopohl and K. Scharnberg, Solid State Commun. **22**, 371

(1977).
[41] W. L. McMillan, Phys. Rev. **175**, 537 (1968).
[42] F. Giubileo, D. Roditchev, W. Sacks, R. Lamy, and J. Klein, Europhys. Lett. **58**, 764 (2002).
[43] C. L. Huang, J.-Y. Lin, Y. T. Chang, C. P. Sun, H. Y. Shen, C. C. Chou, H. Berger, T. K. Lee, and H. D. Yang, Phys. Rev. B **76**, 212504 (2007).
[44] A. Bussmann-Holder, R. Micnas, and A. R. Bishop, Eur. Phys. J. B **37**, 345 (2003).
[45] The high-frequency noise of the voltage source or a "jitter" due to an insufficient filtering may also introduce an effective electronic temperature higher than the bath temperature.
[46] J. Tersoff and D. R. Hamann, Phys. Rev. B **31**, 805 (1985).
[47] N. Bergeal, V. Dubost, Y. Noat, W. Sacks, D. Roditchev, N. Emery, C. Hérold, J.-F. Marêché, P. Lagrange, and G. Loupias, Phys. Rev. Lett. **97**, 077003 (2006).
[48] R. S. Gonnelli, D. Daghero, D. Delaude, M. Tortello, G. A. Ummarino, V. A. Stepanov, J. S. Kim, R. K. Kremer, A. Sanna, G. Profeta, and S. Massidda, Phys. Rev. Lett. **100**, 207004 (2008).
[49] R. C. Dynes, V. Narayanamurti, and J. P. Garno, Phys. Rev. Lett. **41**, 1509 (1978).
[50] T. Proslier, J. F. Zasadzinski, L. Cooley, C. Antoine, J. Moore, J. Norem, M. Pellin, and K. E. Gray, Appl. Phys. Lett. **92**, 212505 (2008).
[51] Y. Jing, S. Lei, W. Yue, X. Zhi-Li, and W. Hai-Hu, Chin. Phys. B **17**, 2229 (2008).
[52] J. D. Fletcher, A. Carrington, P. Diener, P. Rodière, J. P. Brison, R. Prozorov, T. Olheiser, and R. W. Giannetta, Phys. Rev. Lett. **98**, 057003 (2007).
[53] Note that in all these works the interband QP scattering effects were not considered.
[54] Boaknin *et al.* (Ref. 22) deduced the gap ratio $\Delta/\Delta^* \sim 3$ between the large and small gap using $\Delta \sim v_F/\xi$ and assuming the same Fermi velocity in each band. The latter hypothesis is questionable, since the Fermi velocity might vary depending on the Fermi sheet, and also inside a given Fermi sheet. Some recent photoemission measurements, T. Kiss, T. Yokoya, A. Chainani, S. Shin, T. Hanaguri, M. Nohara, and H. Takagi, Nat. Phys. **3**, 720 (2007), demonstrated that the Fermi velocity varies from 0.56 to 3.22 eV/Å in 2H-$NbSe_2$ This could explain the discrepancy in the ratio Δ_L/Δ_S found in Boaknin *et al.* (Ref. 22) as compared to other reports.
[55] It is probably the case in Ba_8Si_{46}, Y. Noat, T. Cren, P. Toulemonde, A. San Miguel, F. Debontridder, V. Dubost, and D. Roditchev, Phys. Rev. B **81**, 104522 (2010).
[56] I. Guillamón, H. Suderow, S. Vieira, L. Cario, P. Diener, and P. Rodière, Phys. Rev. Lett. **101**, 166407 (2008).